Barrier-Function-based Distributed Adaptive Control of Nonlinear CAVs with Parametric Uncertainty and Full-state Constraint

Yang Zhu[a], Feng Zhu[a,*]

[a]*School of Civil and Environmental Engineering, Nanyang Technological University, Singapore*

Abstract

The platoon control of connected and automated vehicles (CAVs) is an emerging problem and has become a hot topic in transportation research. Most of the existing results are based on second-order or third-order linear vehicular dynamics. They ignore either the actuator internal kinetics or vehicular inherent nonlinearity, and the linearization requires a complete priori knowledge of plant parameters and may not be easy to implement in practice. In order to overcome these shortcomings, this paper concentrates on third-order nonlinear vehicular plants with parametric uncertainty and full-state constraint. Different from the popular linear-matrix-inequality (LMI) robust control and model predictive control (MPC), this paper proposes a barrier-function-based distributed adaptive backstepping control scheme. The third-order nonlinear vehicle models are considered, uncertain parameters are identified on-line, full-state constraints are not violated, and the tracking control objectives are established. Simulation studies are carried out to verify the effectiveness of the developed control design.

Keywords: Distributed, Adaptive, Connected and Automated Vehicles, Parametric Uncertainty, State Constraint.

1. Introduction

With the rapid development of advanced technologies in the fields of wireless communication and intelligent automation, research on connected and automated vehicles (CAVs) is booming and has attracted widespread attention from scholars around the world Bian et al. (2019); Ge and Orosz (2014); Li et al. (2018); Sun and Yin (2019). Although CAVs have great potential to improve traffic safety, efficiency, and sustainability, the development of CAVs is still full of challenges. Among the many technical challenges of CAVs, an important and popular research topic is the platoon control of the longitudinal movement of CAVs based on vehicle-to-vehicle (V2V) communication.

Generally, the longitudinal control of CAVs platoon is to regulate a chain of vehicles to an ideal steady state, in which the following vehicles track the leading vehicle at a desirable velocity while maintaining a safe and comfortable inter-vehicle distance. From a networked perspective, the recent publication of Li et al. (2017a) gives an insightful review on CAVs systems, in which the platoon control problem is divided into five interrelated parts. For readers' convenience, these five parts with representative examples are summarized in Table 1.

Based on our previous work on CAVs and traffic networks (Zhu and Zhu , 2018; Zhu and Ukkusuri, 2017, 2015), this paper further investigates more complex CAVs systems. In this paper, the third-order nonlinear vehicular dynamics, the uncertainty in vehicle parameters, and the constraint on vehicle full-state are taken into account together. The control design of such a combined problem is challenging and has not been addressed in existing literature. Intuitively, the longitudinal dynamics of CAVs is a typical class of parametric-strict-feedback systems with a relative degree equal to two or three. The control objective is to track the time-varying velocity of a leading vehicle and maintain the desired platoon formation, which is a standard tracking or regulation problem. Therefore,

*Corresponding author.

E-mail address: zhuyang@ntu.edu.sg, zhufeng@ntu.edu.sg

Table 1: Literature on the platoon control problem of CAVs

ⓐ Vehicular Dynamics: the physical systems to represent vehicle longitudinal motion.
• "position-velocity" second-order linear model (Feng et al., 2018; Filho et al., 2017; Zhai et al., 2018)
• "position-velocity" second-order nonlinear model (Li and Yang et al., 2015, 2014; Swaroop et al., 2001)
• "position-velocity-acceleration" third-order linear model (Petrillo et al., 2018; Salvi et al., 2017)
• "position-velocity-force" third-order nonlinear model (Zheng et al., 2017a; Zhu and Zhu , 2018)
• "position-velocity-acceleration" third-order nonlinear model (Guo and Yue, 2012)
ⓑ Vehicle-to-Vehicle (V2V) Communication: the communication mode to describe information interaction among CAVs.
• "predecessor-following" (PF) type (Li et al., 2017a)
• "bi-directional" (BD) type (Li et al., 2017a)
• "predecessor-leader-following" (PLF) type (Li et al., 2017a)
• "two-predecessor-following" (TPF) type (Chehardoli and Ghasemi, 2018)
• "two-predecessor-leader-following" (TPLF) type (Zhai et al., 2018)
ⓒ Spacing policy: the formation regulation to govern inter-vehicle distance.
• "constant-distance" (CD) policy (Gong et al., 2016; Petrillo et al., 2018; Zheng et al., 2017b)
• "constant-time-headway" (CTH) policy (Salvi et al., 2017)
ⓓ Stability: the criterion to evaluate platoon performance.
• platoon stability (Li et al., 2017a; Ploeg et al., 2014)
• string stability (Ploeg et al., 2014)
ⓔ Control: the feedback law for a vehicle platoon to achieve expected goals.
• cooperative linear control (Li et al., 2017a; Petrillo et al., 2018; Salvi et al., 2017)
• linear-matrix-inequality-based (LMI) H_∞ control (Li et al., 2017b; Zheng et al., 2017b)
• sliding mode control (SMC) (Gao et al., 2018)
• model predictive control (MPC) (Gong et al., 2018; Zheng et al., 2017a; Zhou et al., 2017)

the backstepping approach (Krstic et al., 1995; Zhu et al., 2018a,b, 2017, 2015) is well suitable for solving the platoon control of CAVs. Specifically, this paper proposes a distributed backstepping control design to solve the above combined problem of CAVs. The contributions of this paper are highlighted as follows:

- **Third-order Nonlinear Vehicular Plant**: A large number of existing literatures focus on the "position-velocity" second-order linear vehicular dynamics (Feng et al., 2018; Gong et al., 2016; Zhai et al., 2018). As stated in (Li et al., 2017a), the seconder-order linear models treat acceleration directly as the control input and may be too simple to accurately capture the features of the vehicle's internal engine. Omitting the inherent nonlinearity of vehicular dynamics may lead to instability in the real-world driving environment. One improvement in vehicle modeling is the popular "position-velocity-acceleration" third-order linear models, on which a large number of cooperative control and optimization approaches are based (Li et al., 2017a; Ploeg et al., 2014; Petrillo et al., 2018; Salvi et al., 2017; Zhu and Zhao et al., 2018). Unfortunately, the third-order linear models are simplified from the nonlinear systems by exact feedback linearization, which requires a perfect prior knowledge of the vehicular dynamics (see Remark 1 in Section 2). Different from the above two types of models, this paper concentrates on third-order nonlinear vehicular dynamics (Guo and Yue, 2012; Li et al., 2017a; Sheikholeslam et al., 1993; Zheng et al., 2017a). Third-order nonlinear systems not only consider the inherent nonlinearity of the vehicular dynamic, but also the internal kinetics of the actuator, which are much closer to actual vehicles.

- **Parametric Uncertainty**: Given the large number of vehicles in the actual traffic stream and the heterogeneity of vehicles, it is difficult to collect exact information on the dynamics of every individual vehicle. Therefore, the uncertainty in plant parameters is an inevitable element of control design. In particular, when part or all of vehicular parameters are unknown, the widely-used linear systems cannot be obtained by linearization (see Remark 1 in Section 2). Chehardoli and Ghasemi (2018) focus on the second-order uncertain vehicular dynamics, but a direct extension to higher-order models does not seem promising. Zheng et al. (2017b) and Li et al. (2017b) employ the H_∞ control for linear systems to address the uncertainty due to bounded external disturbance or modeling error, but the approach cannot be applied to the parametric uncertainty (which is usually multiplied by system states and therefore cannot be treated as bounded). Li

et al. (2017c) and Zhu and Zhao et al. (2018) apply the robust and adaptive method, respectively, but they look at the third-order linearized systems with the uncertainty only in the engine time lag. The third-order nonlinear systems are considered by Gao et al. (2018) and the adaptive slide mode control is utilized, but some parameters are still required to be known to designers. In this paper, we consider the third-order nonlinear systems, assuming all vehicular parameters unknown, allowing for uncertainties in both control coefficients and plant parameters, which is not an easy task even for nonlinear control theory.

- **Full-state Constraint**: Another practical contribution of this paper is that the constraint on vehicular states is incorporated. Specifically, the state constraint considers the minimum safety distance and the maximum distance to ensure V2V communication, the different speed limits on freeways and school roads, and the maximum deceleration/acceleration of driving comfort. An effective method to deal with the state constraint is model predictive control (MPC), also called receding horizon control. MPC is an optimization-based method, in which the control input sequence is derived from the cost minimization subject to state and input constraints. From the view that MPC can deal with constraints on both plant state and control input, MPC seems to be better than backstepping. However, MPC has its own considerable shortcomings, especially when it is applied to large-scale vehicles in a platoon. Linear MPC in (Filho et al., 2017; Gong et al., 2018; Wang et al., 2014a,b; Zhai et al., 2018; Zhou et al., 2017) all focus on the second-order linear systems, which may not adequately reflect the high-order nonlinearity of vehicle dynamics (nonlinear MPC is much more complicated and challenging). In addition, to achieve a desirable equilibrium for all following vehicles, Zhou et al. (2017) requires all followers to monitor the leader's real-time behavior, which involves long-range heavy-volume data communication. To ensure the existence of an optimal solution, the inequalities (14) in Zhai et al. (2018) request a strict order of velocities' constraints, which is a strong restriction. Zheng et al. (2017a) proposes the distributed MPC for third-order nonlinear systems but only the input saturation is considered. In this paper, to avoid the aforementioned potential shortcomings of MPC , we adopt a totally different method (barrier-fucntion-based backstepping) to handle the third-order vehicular model with nonlinearity and full-state constraints.

- **Simple Communication Type**: To the authors' best knowledge, this paper is the first attempt to integrate the third-order vehicular nonlinearity, parametric uncertainty and full-state constraint, in solving the platoon control problem. A very recent publication by Chen et al. (2018) utilizes a Min-Max MPC to deal with both parametric uncertainty and state constraint, but it is still based on the third-order linearized systems. Another shortcoming is that the centralized MPC in Chen et al. (2018) also requires the leader to collect/send information from/to all followers, which needs large-volume communication over long distance, often resulting in delays and dropouts. Unlike MPC, the backstepping control of this paper employs the simple V2V communication style, i.e., the bi-directional (BD) type. It only requires short-range information communication, neither requiring the leader's data to be transmitted to every platoon member, nor requiring one member to collect data from all of its predecessors and followers. This short-distance and low-volume BD type information exchange greatly reduces the effect of the communication-delay-dropout and makes it to implement in practice. In fact, in this paper, if one vehicle is equipped with sensors to measure the states (position-velocity-acceleration) of its nearest predecessor and successor, the control design can work without communication (see Remark 3 in Section 3).

The rest of the paper is organized as follows. In Section 2.1, the third-order nonlinear vehicular dynamics with parametric uncertainty and full-state constraint, as well as the control objectives are presented. Its relationship with other widely-used linearized models is discussed in Section 2.2. The barrier-function-based transformation to address state constraint is introduced in Section 2.3. The distributed backstepping-based adaptive control algorithm is proposed to deal with vehicular parametric uncertainty in Section 3.1, whereas both parameter uncertainty and state constraint are addressed in Section 3.2. In Section 4, the simulation study is performed to test the feasibility of the control scheme. Finally, Section 5 concludes the paper.

2. Problem Formulation

2.1. Third-order Nonlinear Vehicular Dynamics with Parametric Uncertainty and Full-state Constraint

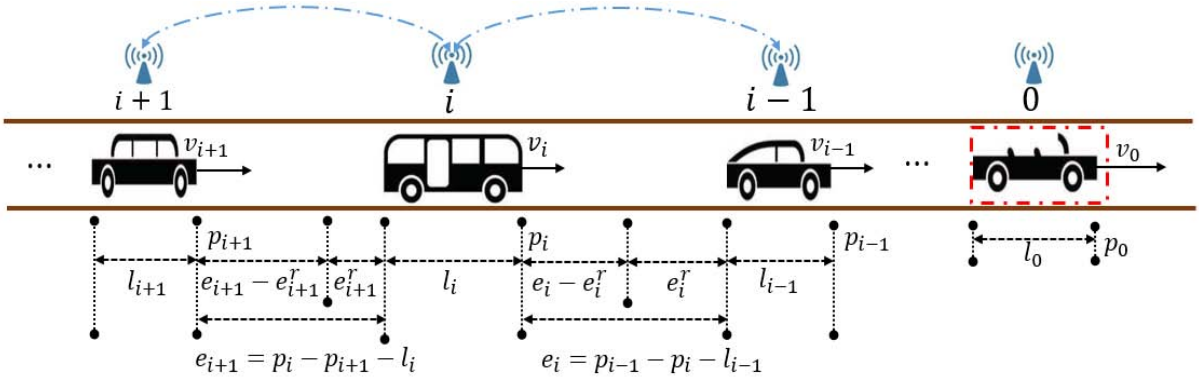

Figure 1: Longitudinal Motion of a Platoon of $n+1$ CAVs

Consider a platoon of $n+1$ CAVs on a road as shown in Fig. 1. The dynamics of an individual vehicle i in the platoon is described by a general class of third-order nonlinear model as follows:

• **"Position-Velocity-Force" Third-order Nonlinear Model** (Li et al., 2017a; Sheikholeslam et al., 1993; Ioannou et al., 1993; Swaroop et al., 1994; Godbole et al., 1994; Zheng et al., 2017a)

$$\dot{p}_i(t) = v_i(t) \tag{1}$$

$$\dot{v}_i(t) = \frac{1}{m_i}F_i(t) - \frac{K_{di}}{m_i}v_i^2(t) - \frac{d_{mi}}{m_i} \tag{2}$$

$$\dot{F}_i(t) = \frac{1}{\tau_i}u_i(t) - \frac{1}{\tau_i}F_i(t), \quad i = 1, 2, \cdots, n \tag{3}$$

where $p_i(t)$ and $v_i(t)$ are the position and velocity of the ith vehicle, respectively; $F_i(t)$ is the driving/braking force generated by the ith vehicle's engine; $u_i(t)$ denotes the throttle/brake pedal command, which is treated as the control input; Equation (2) satisfies Newton's second law of motion. Equation (3) represents the ith vehicle's internal engine dynamics. The vehicular constant parameters are listed in Table 2. Given the large and heterogeneous variety of vehicles in a complex traffic environment, the information collection of vehicular dynamics for each vehicle may be impractical in practice. Therefore, it is reasonable to assume that the plant parameters in Table 2 are unknown.

Table 2: Vehicular Parameters

Parameters of Vehicle i	Unit	Range
Vehicle mass m_i	kg	$950 \sim 1750$
Engine time lag τ_i	s	$0.2 \sim 0.9$
Aerodynamic drag coefficient K_{di}	$N\frac{s^2}{m^2}$	$0.1 \sim 0.5$
Mechanical drag d_{mi}	N	$0 \sim 110$

Introducing the variable substitution $a_i(t) = \dot{v}_i(t)$, taking the time derivatives on both sides of (2), and expressing $F_i(t)$ in terms of $v_i(t)$ and $a_i(t)$, we get the equivalent normalization of (1)-(3) as follows:

• **"Position-Velocity-Acceleration" Third-order Nonlinear Model** (Guo and Yue, 2012; Sheikholeslam et al., 1993)

$$\begin{aligned}
\dot{p}_i(t) &= v_i(t) && (4)\\
\dot{v}_i(t) &= a_i(t) && (5)\\
\dot{a}_i(t) &= \frac{1}{m_i\tau_i}u_i(t) - \frac{2K_{di}}{m_i}v_i(t)a_i(t) - \frac{1}{\tau_i}\left(a_i(t) + \frac{K_{di}}{m_i}v_i^2(t) + \frac{d_{mi}}{m_i}\right) && (6)\\
&= b_i u_i(t) + \varphi_i^T\big(v_i(t), a_i(t)\big)\theta_i, \quad i = 1, 2, \cdots, n && (7)
\end{aligned}$$

where $a_i(t)$ is the acceleration of the ith vehicle. Comparing (4)-(6) with (1)-(3), it is obvious that nonlinear terms appear only in equation (6), which simplifies the analysis and design. Thus the vehicle model of (4)-(7) is of interest to this paper. In addition, (6) can be written compactly as (7), where $b_i = \frac{1}{m_i\tau_i}$ is the control coefficient, $\theta_i = [-\frac{2K_{di}}{m_i}, -\frac{1}{\tau_i}, -\frac{K_{di}}{\tau_i m_i}, -\frac{d_{mi}}{\tau_i m_i}]^T$ is the unknown plant parameter vector, $\varphi_i = [v_i a_i, a_i, v_i^2, 1]^T$ is the known nonlinear state function. As both of the vehicle mass m_i and the engine time lag τ_i are positive, the sign of b_i is assumed to be known, i.e., $\mathrm{sgn}(b_i) = 1$. Specifically, the leading vehicle is assumed to be

$$\begin{aligned}
\dot{p}_0(t) &= v_0(t) && (8)\\
\dot{v}_0(t) &= a_0(t) && (9)\\
\dot{a}_0(t) &= u_0(t) && (10)
\end{aligned}$$

where $u_0(t)$ is a reference control input to drive the leading vehicle at the desired speed $v_0(t)$.

The target of platoon control is to track the leading vehicle's velocity while maintaining a desired inter-vehicle spacing between any two neighboring vehicles. As shown in Fig. 1, the rear-to-bumper inter-vehicle distance between two consecutive vehicles is introduced as the output such that

$$e_i(t) = p_{i-1}(t) - p_i(t) - l_{i-1}, \quad i = 1, 2, \cdots, n \tag{11}$$

where l_i is the length of the ith vehicle. Accordingly, the desirable/reference inter-vehicle distance is denoted by e_i^r. Here we employ the frequently-used constant distance (CD) spacing policy (Gao et al., 2018; Gong et al., 2016; Petrillo et al., 2018), i.e., the reference inter-vehicle spacing e_i^r is a constant. The control objectives are described mathematically as follows,

$$\begin{aligned}
&\lim_{t\to\infty}\big(e_i(t) - e_i^r\big) = \lim_{t\to\infty}\big(p_{i-1}(t) - p_i(t) - l_{i-1} - e_i^r\big) = 0 && (12)\\
&\lim_{t\to\infty}\big(v_i(t) - v_0(t)\big) = 0 && (13)
\end{aligned}$$

In addition to the above-mentioned parametric uncertainty and nonlinearity, vehicular full-state constraints are common in real-world traffic environment. Therefore, the following full-state constraints are expected:

$$\begin{aligned}
\underline{e} < e_i(t) < \overline{e}, &\qquad \overline{e} > \underline{e} > 0 && (14)\\
\underline{v} < v_i(t) < \overline{v}, &\qquad \overline{v} > \underline{v} \geq 0 && (15)\\
-\underline{a} < a_i(t) < \overline{a}, &\qquad \underline{a} > 0, \overline{a} > 0 && (16)
\end{aligned}$$

where $\underline{e}$ and $\overline{e}$ respectively refer to the inter-vehicle minimum distance for safety and the maximum distance for platoon formation and communication; $\underline{v}$ and $\overline{v}$ respectively refer to the lowest and highest speed limits that often occur on freeways and school roads; $-\underline{a}$ and $\overline{a}$ respectively refer to the maximum deceleration and acceleration to ensure driving comfort.

2.2. Failure of Exact Feedback Linearization due to Parametric Uncertainty

Under the assumption that all parameters in Table 2 are known, a popular method to eliminate nonlinearities in (6) is the exact feedback linearization such that

$$u_i(t) = m_i c_i(t) + 2\tau_i K_{di} v_i(t) a_i(t) + K_{di} v_i^2(t) + d_{mi} \tag{17}$$

by which the nonlinear dynamics (4)-(6) are transformed into the widely-used third-order linear systems (Ploeg et al., 2014; Petrillo et al., 2018; Salvi et al., 2017):

$$\dot{p}_i(t) = v_i(t) \tag{18}$$
$$\dot{v}_i(t) = a_i(t) \tag{19}$$
$$\dot{a}_i(t) = \frac{1}{\tau_i} c_i(t) - \frac{1}{\tau_i} a_i(t) \tag{20}$$

where $c_i(t)$ is a new exogenous control input.

Remark 1: Most existing cooperative or distributed linear control/optimization algorithms are based on the linearized model (18)-(20). Once a linear control law $c_i(t)$ for the linear system (18)-(20) is developed, it can be inversely converted to a nonlinear control law $u_i(t)$ for the nonlinear system (4)-(6) by the equality (17). Nevertheless, the linearization technique (17) requires a perfect knowledge of all vehicular parameters, which is why it is called "exact". In other words, if some parameters in Table 2 are unknown, the linear-nonlinear mutual conversion (17) will fail and the subsequent linear methods cannot be applied. A few recent publications (Chen et al., 2018; Li et al., 2017c; Zhu and Zhao et al., 2018) consider the uncertainty in the parameter τ_i of the linearized system (18)-(20). They estimate the uncertain τ_i by a fixed nominal value $\hat{\tau}_i$ with an estimation error $\tilde{\tau}_i = \tau_i - \hat{\tau}_i$ which is required to be bounded and of a small value. Then linear methods can still be applied. However, note that the linear system (18)-(20) is derived from the nonlinear model (4)-(6) by making use of the exact feedback linearization (17). When τ_i is uncertain and replaced by its estimate $\hat{\tau}_i$, the linearization (17) becomes

$$u_i(t) = m_i c_i(t) + 2\hat{\tau}_i K_{di} v_i(t) a_i(t) + K_{di} v_i^2(t) + d_{mi} \tag{21}$$

By substituting (21) into (6), (4)-(6) is transformed to

$$\dot{p}_i(t) = v_i(t) \tag{22}$$
$$\dot{v}_i(t) = a_i(t) \tag{23}$$
$$\dot{a}_i(t) = \frac{1}{\tau_i} c_i(t) - \frac{1}{\tau_i} a_i(t) - \frac{2K_{di}(\tau_i - \hat{\tau}_i)}{m_i \tau_i} v_i(t) a_i(t) \tag{24}$$

which is still a nonlinear system in nature, not a linear system (18)-(20). Especially, by comparing (22)-(24) with (18)-(20), the nonlinear term in (24) should not be regarded as a bounded external disturbance to be handled by LMI robust control (Li et al., 2017b; Zheng et al., 2017b). In contrast, the nonlinear term depends on the system states and therefore cannot be considered bounded when the estimation error $\tau_i - \hat{\tau}_i$ or the product of v_i and a_i is large. Therefore, the recently published control designs to address the uncertainty of only τ_i in linearized systems (18)-(20) may not be applicable to actual vehicles. More importantly, when other parameters m_i, K_{di} and d_{mi} in Table 2 are also uncertain, the linearization (17) is completely unavailable, and the nonlinear control problem of uncertain nonlinear systems (4)-(7) is more challenging.

2.3. Barrier-Function-based Invertible Transformation to address Full-state Constraint

Different from classic linear MPC to deal with full-state constraints in (14)-(16), we consider the invertible transformation of barrier functions as follows, (the time notation (t) is omitted for the sake of brevity)

$$e_i = f_e(y_i^e) \quad \Leftrightarrow \quad y_i^e = f_e^{-1}(e_i) \tag{25}$$
$$v_i = f_v(y_i^v) \quad \Leftrightarrow \quad y_i^v = f_v^{-1}(v_i) \tag{26}$$
$$a_i = f_a(y_i^a) \quad \Leftrightarrow \quad y_i^a = f_a^{-1}(a_i) \tag{27}$$

where $f_e(\cdot)$ and $f_e^{-1}(\cdot)$, $f_v(\cdot)$ and $f_v^{-1}(\cdot)$, $f_a(\cdot)$ and $f_a^{-1}(\cdot)$ are inverse functions of each other. Moreover, they are smoothly continuous and strictly increasing in their respective arguments, and satisfy

$$\begin{cases} \underline{e} < f_e(y_i^e) < \overline{e} \\ \lim\limits_{y_i^e \to +\infty} f_e(y_i^e) = \overline{e} \\ \lim\limits_{y_i^e \to -\infty} f_e(y_i^e) = \underline{e} \end{cases} \quad \begin{cases} \underline{v} < f_v(y_i^v) < \overline{v} \\ \lim\limits_{y_i^v \to +\infty} f_v(y_i^v) = \overline{v} \\ \lim\limits_{y_i^v \to -\infty} f_v(y_i^v) = \underline{v} \end{cases} \quad \begin{cases} -\underline{a} < f_a(y_i^a) < \overline{a} \\ \lim\limits_{y_i^a \to +\infty} f_a(y_i^a) = \overline{a} \\ \lim\limits_{y_i^a \to -\infty} f_a(y_i^a) = -\underline{a} \end{cases} \tag{28}$$

$$\begin{cases} -\infty < f_e^{-1}(e_i) < +\infty \\ \lim\limits_{e_i \to \overline{e}} f_e^{-1}(e_i) = +\infty \\ \lim\limits_{e_i \to \underline{e}} f_e^{-1}(e_i) = -\infty \end{cases} \quad \begin{cases} -\infty < f_v^{-1}(v_i) < +\infty \\ \lim\limits_{v_i \to \overline{v}} f_v^{-1}(v_i) = +\infty \\ \lim\limits_{v_i \to \underline{v}} f_v^{-1}(v_i) = -\infty \end{cases} \quad \begin{cases} -\infty < f_a^{-1}(y_i^a) < +\infty \\ \lim\limits_{a_i \to \overline{a}} f_a^{-1}(a_i) = +\infty \\ \lim\limits_{a_i \to -\underline{a}} f_a^{-1}(a_i) = -\infty \end{cases} \tag{29}$$

Remark 2: If initial states satisfy $e_i(0) \in (\underline{e}, \overline{e})$, $v_i(0) \in (\underline{v}, \overline{v})$ and $a_i(0) \in (-\underline{a}, \overline{a})$, then $y_i^e(0)$, $y_i^v(0)$ and $y_i^a(0)$ are bounded. If $y_i^e(t)$, $y_i^v(t)$ and $y_i^a(t)$, $\forall t > 0$ can be further stabilized to be bounded, then $e_i = f_e(y_i^e)$, $v_i = f_v(y_i^v)$, $a_i = f_a(y_i^a)$ satisfy the state-constraint (14)-(16) for any $t > 0$. Thus, the challenging control problem with full-state constraint is converted into the relatively simple control problem that only requires state boundedness.

Note that constraints (14)-(16) are asymmetric. To transform the asymmetric constraints to symmetric constraints, (14)-(16) are rewritten as follows,

$$\left| e_i(t) - \frac{\overline{e} + \underline{e}}{2} \right| < \frac{\overline{e} - \underline{e}}{2}, \quad \left| v_i(t) - \frac{\overline{v} + \underline{v}}{2} \right| < \frac{\overline{v} - \underline{v}}{2}, \quad \left| a_i(t) - \frac{\overline{a} - \underline{a}}{2} \right| < \frac{\overline{a} + \underline{a}}{2} \tag{30}$$

Following the structure of above inequalities, the barrier-function-based invertible transformations (25)-(27) are as follows,

$$\begin{cases} e_i = f_e(y_i^e) = \frac{\overline{e}+\underline{e}}{2} + \frac{\overline{e}-\underline{e}}{2} \tanh(y_i^e) \\ y_i^e = f_e^{-1}(e_i) = \frac{1}{2} \ln \frac{e_i - \underline{e}}{\overline{e} - e_i} \end{cases} \quad \begin{cases} v_i = f_v(y_i^v) = \frac{\overline{v}+\underline{v}}{2} + \frac{\overline{v}-\underline{v}}{2} \tanh(y_i^v) \\ y_i^v = f_v^{-1}(v_i) = \frac{1}{2} \ln \frac{v_i - \underline{v}}{\overline{v} - v_i} \end{cases} \quad \begin{cases} a_i = f_a(y_i^a) = \frac{\overline{a}-\underline{a}}{2} + \frac{\overline{a}+\underline{a}}{2} \tanh(y_i^a) \\ y_i^a = f_a^{-1}(a_i) = \frac{1}{2} \ln \frac{a_i + \underline{a}}{\overline{a} - a_i} \end{cases} \tag{31}$$

where the hyperbolic tangent function $\tanh(\delta) = \frac{\exp(\delta) - \exp(-\delta)}{\exp(\delta) + \exp(-\delta)}$ for $\delta \in (-\infty, \infty)$. As shown in Fig. 2, it is obvious that (28)-(29) are satisfied and we have

$$e_i \in (\underline{e}, \overline{e}) \quad \Leftrightarrow \quad y_i^e \in (-\infty, +\infty) \tag{32}$$
$$v_i \in (\underline{v}, \overline{v}) \quad \Leftrightarrow \quad y_i^v \in (-\infty, +\infty) \tag{33}$$
$$a_i \in (-\underline{a}, \overline{a}) \quad \Leftrightarrow \quad y_i^a \in (-\infty, +\infty) \tag{34}$$

It is also obvious that f_e and f_e^{-1}, f_v and f_v^{-1}, f_a and f_a^{-1}, are smooth and strictly increasing. This can be easily checked by their partial derivatives.

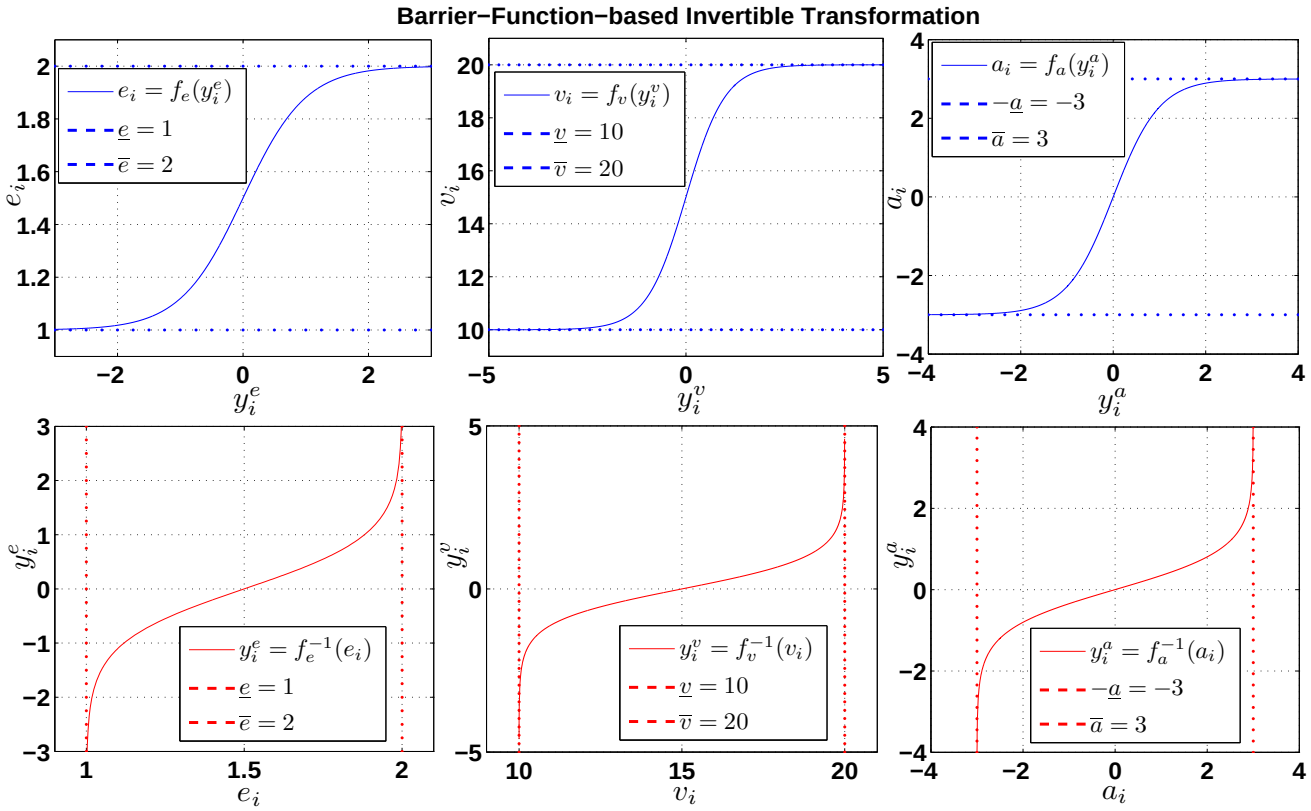

Figure 2: Demonstration of Invertible Transformation by the Barrier-Function $\tanh(\cdot)$ and $\ln(\cdot)$

Combining (4)-(7) with (25)-(27), the dynamics of (y_i^e, y_i^v, y_i^a) is calculated as follows,

$$\dot{y}_i^e = \frac{\partial f_e^{-1}}{\partial e_i}(e_i) \cdot \left(v_{i-1} - f_v(y_i^v)\right) = g_i^e(y_i^e, y_{i-1}^v, y_i^v) \tag{35}$$

$$\dot{y}_i^v = \frac{\partial f_v^{-1}}{\partial v_i}(v_i) \cdot f_a(y_i^a) = g_i^v(y_i^v, y_i^a) \tag{36}$$

$$\dot{y}_i^a = \frac{\partial f_a^{-1}}{\partial a_i}(a_i) \cdot (b_i u_i + \varphi_i^T \theta_i) = g_i^a(y_i^a) b_i u_i + \phi_i^a(y_i^v, y_i^a)^T \theta_i \tag{37}$$

3. Distributed Adaptive Control of CAVs with Parametric Uncertainty and Full-State Constraint

3.1. Distributed Backstepping Control of CAVs with Parametric Uncertainty and Free State

To help readers better understand the proposed adaptive backstepping algorithm, in this section we consider the relatively simple case of CAVs with parametric uncertainty but no state restriction, whereas the more challenging case will be covered in the next section. It is not hard to find the vehicular dynamics (4)-(7) with unknown parameters $b_i = \frac{1}{m_i \tau_i}$ and $\theta_i = [-\frac{2K_{di}}{m_i}, -\frac{1}{\tau_i}, -\frac{K_{di}}{\tau_i m_i}, -\frac{d_{mi}}{\tau_i m_i}]^T$ is a typical third-order parametric-strict-feedback nonlinear system. Moreover, the control objective (12)-(13) is attributed to the standard time-varying trajectory tracking problem. Therefore, the backstepping method (Krstic et al., 1995) is a perfect fit for solving the problem. To overcome the parametric uncertainty and nonlinearity in the vehicular dynamics (4)-(7), utilizing the backstepping concept by (Krstic et al., 1995; Zhu et al., 2017), a distributed adaptive control scheme is proposed as follows,

• **Coordinate Change**

$$
\begin{aligned}
z_{1i} &= e_i - e_i^r = p_{i-1} - p_i - l_{i-1} - e_i^r && (38)\\
z_{2i} &= v_{i-1} - v_i - \alpha_{1i} && (39)\\
z_{3i} &= a_{i-1} - a_i - \alpha_{2i}, \quad i = 1, \cdots, n && (40)
\end{aligned}
$$

where α_{1i} and α_{2i} are virtual controls to be designed below.

• **Control Law**

$$\alpha_{1i} = -c_i z_{1i} \tag{41}$$

$$\alpha_{2i} = -z_{1i} - c_i z_{2i} + \frac{\partial \alpha_{1i}}{\partial p_{i-1}} v_{i-1} + \frac{\partial \alpha_{1i}}{\partial p_i} v_i, \quad i = 1, \cdots, n \tag{42}$$

$$\alpha_{31} = -z_{21} - c_1 z_{31} - u_0 + \varphi_1^T \hat{\theta}_1 + \frac{\partial \alpha_{21}}{\partial p_0} v_0 + \frac{\partial \alpha_{21}}{\partial p_1} v_1 + \frac{\partial \alpha_{21}}{\partial v_0} a_0 + \frac{\partial \alpha_{21}}{\partial v_1} a_1 \tag{43}$$

$$\alpha_{3i} = -z_{2i} - c_i z_{3i} - \hat{b}_{i-1} u_{i-1} - \varphi_{i-1}^T \hat{\theta}_{i-1} + \varphi_i^T \hat{\theta}_i + \frac{\partial \alpha_{2i}}{\partial p_{i-1}} v_{i-1} + \frac{\partial \alpha_{2i}}{\partial p_i} v_i + \frac{\partial \alpha_{2i}}{\partial v_{i-1}} a_{i-1} + \frac{\partial \alpha_{2i}}{\partial v_i} a_i, \quad i = 2, \cdots, n \tag{44}$$

$$u_i = -\hat{\varrho}_i \alpha_{3i}, \quad i = 1, \cdots, n \tag{45}$$

where $\hat{\theta}_i$ is the estimate of θ_i with error $\tilde{\theta}_i = \theta_i - \hat{\theta}_i$, $\hat{b}_i$ is the estimate of b_i with error $\tilde{b}_i = b_i - \hat{b}_i$, $\hat{\varrho}_i$ is the estimate of $\varrho_i = \frac{1}{b_i}$ with error $\tilde{\varrho}_i = \varrho_i - \hat{\varrho}_i$, $c_i > 0$ is a design coefficient to be specified by designers.

• **Parameter Update Law**

$$
\begin{aligned}
\dot{\hat{\theta}}_i &= \gamma_i \varphi_i (z_{3,i+1} - z_{3i}), \quad i = 1, \cdots, n-1 && (46)\\
\dot{\hat{\theta}}_n &= -\gamma_n \varphi_n z_{3n} && (47)\\
\dot{\hat{b}}_i &= \gamma_i u_i z_{3,i+1}, \quad i = 1, \cdots, n-1 && (48)\\
\dot{\hat{\varrho}}_i &= -\gamma_i \mathrm{sgn}(b_i) \alpha_{3i} z_{3i}, \quad i = 1, \cdots, n && (49)
\end{aligned}
$$

where $\gamma_i > 0$ is a design coefficient.

Theorem 1: Consider the closed-loop system consisting of the CAVs dynamics (4)-(10) with the output (11) and the uncertain parameters in Table 2, the coordinate change (38)-(40), the control law (41)-(45) and the parameter update law (46)-(49), the control objectives of (12)-(13) are guaranteed.

Proof: To help readers who may not be familiar with backstepping to better understand the control scheme in (38)-(49), we take vehicles $i-1$ and i as an example to illustrate the control design step by step.

Step 1 of Vehicle i. It is easy to check that the coordinate change z_{1i} in (38) defines the spacing error between the actual inter-vehicle rear-to-bump distance and its desired value. The control goal is to converge z_{1i} to zero. We calculate the time-derivative of z_{1i} of (38) along (4) such that

$$\dot{z}_{1i} = \dot{p}_{i-1} - \dot{p}_i = v_{i-1} - v_i \tag{50}$$

in which there is no control input that can be used to stabilize z_{1i}. To overcome this, the coordinate change (39) is introduced. Then (50) becomes

$$\dot{z}_{1i} = z_{2i} + \alpha_{1i} \tag{51}$$

where α_{1i} is a virtual control to be designed. If α_{1i} is chosen as (41), then

$$\dot{z}_{1i} = -c_i z_{1i} + z_{2i} \tag{52}$$

The z_{1i} system (52) is input-to-state stable with respect to z_{2i}. If z_{2i} converges to zero, the system (52) is asymptotically stable.

Step 2 of Vehicle i. This step is to let z_{2i} decay to zero. Note that α_{1i} in (41) is dependent on p_{i-1} and p_i. The time-derivative of z_{2i} of (39) along (5) is calculated as

$$\begin{aligned} \dot{z}_{2i} &= \dot{v}_{i-1} - \dot{v}_i - \dot{\alpha}_{1i} \\ &= a_{i-1} - a_i - \frac{\partial \alpha_{1i}}{\partial p_{i-1}} v_{i-1} - \frac{\partial \alpha_{1i}}{\partial p_i} v_i \end{aligned} \tag{53}$$

Similar to (50), there is no input in (53). To produce a virtual control to stabilize z_{2i}, by the coordinate change (40), the dynamics (53) becomes

$$\dot{z}_{21} = z_{3i} + \alpha_{2i} - \frac{\partial \alpha_{1i}}{\partial p_{i-1}} v_{i-1} - \frac{\partial \alpha_{1i}}{\partial p_i} v_i \tag{54}$$

If the virtual control α_{2i} is selected as (42), then (54) becomes

$$\dot{z}_{2i} = -z_{1i} - c_i z_{2i} + z_{3i} \tag{55}$$

As in step 1, the variable z_{1i} converges to zero if z_{2i} converges to zero. Thus it is obvious that the z_{2i} system (55) is input-to-state stable with respect to z_{3i}.

Step 3 of Vehicle i. This step is to let z_{3i} decay to zero. Note that α_{2i} in (42) is dependent on p_{i-1}, p_i, v_{i-1} and v_i. The time-derivative of z_{3i} of (40) along (7) is calculated as

$$\begin{aligned} \dot{z}_{3i} &= \dot{a}_{i-1} - \dot{a}_i - \dot{\alpha}_{2i} \\ &= b_{i-1} u_{i-1} + \varphi_{i-1}^T \theta_{i-1} - b_i u_i - \varphi_i^T \theta_i - \frac{\partial \alpha_{2i}}{\partial p_{i-1}} v_{i-1} - \frac{\partial \alpha_{2i}}{\partial p_i} v_i - \frac{\partial \alpha_{2i}}{\partial v_{i-1}} a_{i-1} - \frac{\partial \alpha_{2i}}{\partial v_i} a_i \end{aligned} \tag{56}$$

Since the actual control input u_i appears, no more coordinate change is needed. By designing the actual control as (45), the third term on the right side of (56) becomes $-b_i u_i = b_i \hat{\varrho}_i \alpha_{3i} = b_i(\varrho_i - \tilde{\varrho}_i)\alpha_{3i} = \alpha_{3i} - b_i \tilde{\varrho}_i \alpha_{3i}$. Furthermore, by designing α_{3i} as (44) to remove redundant terms in (56), then (56) becomes

$$\dot{z}_{3i} = -z_{2i} - c_i z_{3i} - b_i \tilde{\varrho}_i \alpha_{3i} + \tilde{b}_{i-1} u_{i-1} + \varphi_{i-1}^T \tilde{\theta}_{i-1} - \varphi_i^T \tilde{\theta}_i \tag{57}$$

Lyapunov-based Stability Analysis. Build the Lyapunov candidate for the closed-loop system of vehicle i as

$$V_i = \frac{1}{2} z_{1i}^2 + \frac{1}{2} z_{2i}^2 + \frac{1}{2} z_{3i}^2 + \frac{|b_i|}{2\gamma_i} \tilde{\varrho}_i^2 + \frac{1}{2\gamma_{i-1}} \tilde{b}_{i-1}^2 + \frac{1}{2\gamma_{i-1}} \tilde{\theta}_{i-1}^T \tilde{\theta}_{i-1} + \frac{1}{2\gamma_i} \tilde{\theta}_i^T \tilde{\theta}_i \tag{58}$$

Taking time derivative of (58) along the dynamics of the closed-loop system (52), (55) and (57), we have

$$\begin{aligned}\dot{V}_i &= z_{1i}\left(-c_i z_{1i}+z_{2i}\right)+z_{2i}\left(-z_{1i}-c_i z_{2i}+z_{3i}\right)+z_{3i}\left(-z_{2i}-c_i z_{3i}-b_i\tilde{\varrho}_i\alpha_{3i}+\tilde{b}_{i-1}u_{i-1}+\varphi_{i-1}^T\tilde{\theta}_{i-1}-\varphi_i^T\tilde{\theta}_i\right)\\ &\quad -\frac{|b_i|}{\gamma_i}\tilde{\varrho}_i\dot{\tilde{\varrho}}_i-\frac{1}{\gamma_{i-1}}\tilde{b}_{i-1}\dot{\tilde{b}}_{i-1}-\frac{1}{\gamma_{i-1}}\tilde{\theta}_{i-1}^T\dot{\tilde{\theta}}_{i-1}-\frac{1}{\gamma_i}\tilde{\theta}_i^T\dot{\tilde{\theta}}_i \qquad (59)\\ &= -c_i(z_{1i}^2+z_{2i}^2+z_{3i}^2)-\frac{|b_i|}{\gamma_i}\tilde{\varrho}_i\left(\dot{\tilde{\varrho}}_i+\gamma_i\mathrm{sgn}(b_i)\alpha_{3i}z_{3i}\right)-\frac{1}{\gamma_{i-1}}\tilde{b}_{i-1}\left(\dot{\tilde{b}}_{i-1}-\gamma_{i-1}u_{i-1}z_{3i}\right)\\ &\quad -\frac{1}{\gamma_{i-1}}\tilde{\theta}_{i-1}^T\left(\dot{\tilde{\theta}}_{i-1}-\gamma_{i-1}\varphi_{i-1}z_{3i}\right)-\frac{1}{\gamma_i}\tilde{\theta}_i^T\left(\dot{\tilde{\theta}}_i+\gamma_i\varphi_i z_{3i}\right) \qquad (60)\end{aligned}$$

Then build Lyapunov candidate for the closed-loop systems of the whole vehicle platoon as follows,

$$V = \sum_{i=1}^{n}\left(\frac{1}{2}z_{1i}^2+\frac{1}{2}z_{2i}^2+\frac{1}{2}z_{3i}^2\right)+\sum_{i=1}^{n}\frac{|b_i|}{2\gamma_i}\tilde{\varrho}_i^2+\sum_{i=1}^{n-1}\frac{1}{2\gamma_i}\tilde{b}_i^2+\sum_{i=1}^{n}\frac{1}{2\gamma_i}\tilde{\theta}_i^T\tilde{\theta}_i \qquad (61)$$

From (60), the time derivative of V is calculated as

$$\begin{aligned}\dot{V} &= -\sum_{i=1}^{n}c_i(z_{1i}^2+z_{2i}^2+z_{3i}^2)-\sum_{i=1}^{n}\frac{|b_i|}{\gamma_i}\tilde{\varrho}_i\left(\dot{\tilde{\varrho}}_i+\gamma_i\mathrm{sgn}(b_i)\alpha_{3i}z_{3i}\right)-\sum_{i=1}^{n-1}\frac{1}{\gamma_i}\tilde{b}_i\left(\dot{\tilde{b}}_i-\gamma_i u_i z_{3,i+1}\right)\\ &\quad -\sum_{i=1}^{n-1}\frac{1}{\gamma_i}\tilde{\theta}_i^T\left(\dot{\tilde{\theta}}_i-\gamma_i\varphi_i(z_{3,i+1}-z_{3i})\right)-\frac{1}{\gamma_n}\tilde{\theta}_n^T\left(\dot{\tilde{\theta}}_n+\gamma_n\varphi_n z_{3n}\right) \qquad (62)\end{aligned}$$

By applying parameter update laws (46)-(49) to cancel parameter estimation error terms in (62), it is apparent $\dot{V}$ is non-positive as

$$\dot{V} = -\sum_{i=1}^{n}c_i(z_{1i}^2+z_{2i}^2+z_{3i}^2) \qquad (63)$$

As the time derivative of Lyapunov function is non-positive, V is non-increasing. For $i=1,\cdots,n$, we conclude that z_{1i}, z_{2i}, z_{3i}, $\tilde{\varrho}_i$, $\tilde{b}_i$, $\tilde{\theta}_i$ are all bounded. By applying the well-known LaSalle-Yoshizawa theorem to (63), the asymptotical convergence $\lim_{t\to\infty}z_{1i}=\lim_{t\to\infty}z_{2i}=0$ is obtained, implying (12)-(13) are ensured. Proof of Theorem 1 is completed.

3.2. Distributed Backstepping Control of CAVs with Parametric Uncertainty and State Constraint

In this section, based on Section 3.1, we consider a more difficult case of CAVs with both parametric uncertainty and full-state constraint. As clarified in Section 2.3, the control problem of the system (4)-(7) with the full-state constraint on (e_i, v_i, a_i), is converted to the control problem of the system (35)-(37) with only boundedness requirements on (y_i^e, y_i^v, y_i^a). The backstepping control of the pure-feedback system (35)-(37) is not an easy task because there is no explicit variable that can be used as the virtual control. To overcome this difficulty, as the barrier-functions are well-defined smooth functions (31), the mean value theorem will be utilized to produce the virtual control. Before introducing the control design, we have the following plain assumption,

Assumption 1: The desirable inter-vehicle spacing e_i^r satisfies $\underline{e}<e_i^r<\overline{e}$ for $i=1,\cdots,n$. The reference velocity and acceleration of the leading vehicle satisfy $\underline{v}<v_0(t)<\overline{v}$ and $-\underline{a}<a_0(t)<\overline{a}$.

The distributed adaptive control design to deal with parametric uncertainty and full-state constraint in vehicular dynamics (4)-(7) is presented as follows,

• **Coordinate Change**

$$
\begin{aligned}
z_{1i} &= y_i^e - y_i^{e^r} && (64)\\
z_{2i} &= y_i^v - \alpha_{1i} && (65)\\
z_{3i} &= y_i^a - \alpha_{2i}, \quad i = 1, \cdots, n && (66)
\end{aligned}
$$

where $y_i^{e^r} = f_e^{-1}(e_i^r)$, α_{1i} and α_{2i} are virtual controls similar to (39)-(40).

• Control Law

$$\alpha_{1i} = f_v^{-1}\left(\frac{1}{\frac{\partial f_e^{-1}}{\partial e_i}} c_i z_{1i} + v_{i-1}\right) \tag{67}$$

$$\alpha_{2i} = f_a^{-1}\left(\frac{1}{\frac{\partial f_v^{-1}}{\partial v_i}} \cdot \left(-c_i z_{2i} + \frac{\partial \alpha_{1i}}{\partial p_{i-1}} v_{i-1} + \frac{\partial \alpha_{1i}}{\partial p_i} v_i + \frac{\partial \alpha_{1i}}{\partial v_{i-1}} a_{i-1}\right)\right), \quad i = 1, \cdots, n, \tag{68}$$

$$\alpha_{31} = \frac{1}{\frac{\partial f_a^{-1}}{\partial a_1}} \cdot \left(-c_1 z_{31} + \frac{\partial \alpha_{21}}{\partial a_0} u_0 + \frac{\partial \alpha_{21}}{\partial p_0} v_0 + \frac{\partial \alpha_{21}}{\partial p_1} v_1 + \frac{\partial \alpha_{21}}{\partial v_0} a_0 + \frac{\partial \alpha_{21}}{\partial v_1} a_1\right) - \varphi_1^T \hat{\theta}_1 \tag{69}$$

$$\alpha_{3i} = \frac{1}{\frac{\partial f_a^{-1}}{\partial a_i}} \cdot \left(-c_i z_{3i} + \frac{\partial \alpha_{2i}}{\partial a_{i-1}} \left(\hat{b}_{i-1} u_{i-1} + \varphi_{i-1}^T \hat{\theta}_{i-1}\right) + \frac{\partial \alpha_{2i}}{\partial p_{i-1}} v_{i-1} + \frac{\partial \alpha_{2i}}{\partial p_i} v_i + \frac{\partial \alpha_{2i}}{\partial v_{i-1}} a_{i-1} + \frac{\partial \alpha_{2i}}{\partial v_i} a_i\right) - \varphi_i^T \hat{\theta}_i, \tag{70}$$

$$i = 2, \cdots, n$$

$$u_i = \hat{\varrho}_i \alpha_{3i}, \quad i = 1, \cdots, n \tag{71}$$

where $\frac{1}{\frac{\partial f_e^{-1}}{\partial e_i}}$, $\frac{1}{\frac{\partial f_v^{-1}}{\partial v_i}}$ and $\frac{1}{\frac{\partial f_a^{-1}}{\partial a_1}}$ are reciprocals of $\frac{\partial f_e^{-1}}{\partial e_i}$, $\frac{\partial f_v^{-1}}{\partial v_i}$ and $\frac{\partial f_a^{-1}}{\partial a_1}$, respectively. $\hat{\theta}_i$, $\hat{b}_i$, $\hat{\varrho}_i$ and c_i are defined the same as in Section 3.1.

• **Parameter Update Law**

$$
\begin{aligned}
\dot{\hat{\theta}}_i &= \gamma_i \varphi_i \left(\frac{\partial f_a^{-1}}{\partial a_i} z_{3i} - \frac{\partial \alpha_{2,i+1}}{\partial a_i} z_{3,i+1}\right), \quad i = 1, \cdots, n-1, && (72)\\
\dot{\hat{\theta}}_n &= \gamma_n \varphi_n \frac{\partial f_a^{-1}}{\partial a_n} z_{3n} && (73)\\
\dot{\hat{b}}_i &= -\gamma_i \frac{\partial \alpha_{2,i+1}}{\partial a_i} u_i z_{3,i+1}, \quad i = 1, \cdots, n-1, && (74)\\
\dot{\hat{\varrho}}_i &= -\gamma_i \mathrm{sgn}(b_i) \frac{\partial f_a^{-1}}{\partial a_i} \alpha_{3i} z_{3i}, \quad i = 1, \cdots, n && (75)
\end{aligned}
$$

where γ_i is defined the same as in Section 3.1.

Theorem 2: Under Assumption 1, consider the closed-loop system consisting of nonlinear CAVs dynamics (4)-(10) with the output (11), the uncertain parameters in Table 2 and the full-state constraints of (14)-(16), the barrier-function-based transformation (31), the coordinate change (64)-(66), the control scheme (67)-(71) and the parameter estimate (72)-(75). If initial conditions $\underline{e} < e_i(0) < \overline{e}$, $\underline{v} < v_i(0) < \overline{v}$ and $-\underline{a} < a_i(0) < \overline{a}$ for $i = 1, \cdots, n$ hold, then the control objectives (12)-(13) are achieved, and the full-state constraints (14)-(16) are not violated.

Proof: Similar to the proof of Theorem 1, we take vehicle i as an example to prove Theorem 2 step by step.

Step 1 of Vehicle i. Take time-derivative of z_{1i} of (64) along (35), and use (65),

$$\dot{z}_{1i} = \dot{y}_i^e = \frac{\partial f_e^{-1}}{\partial e_i} \cdot \left(v_{i-1} - f_v(y_i^v)\right) = \frac{\partial f_e^{-1}}{\partial e_i} \cdot \left(v_{i-1} - f_v(\alpha_{1i} + z_{2i})\right) \tag{76}$$

As $f_v(y_i^v)$ is a well-defined smooth function in (31), by the mean value theorem, we have

$$f_v(\alpha_{1i}+z_{2i}) \quad = \quad f_v(\alpha_{1i})+z_{2i}\cdot\frac{\partial f_v}{\partial y_i^v}(y_i^v)\Big|_{y_i^v=\alpha_{1i}+\epsilon z_{2i}} = f_v(\alpha_{1i})+z_{2i}\cdot\frac{\partial f_v}{\partial y_i^v}(\alpha_{1i}+\epsilon z_{2i}) \tag{77}$$

where $\epsilon\in(0,1)$. Substitute (77) into (76), and (76) becomes

$$\dot{z}_{1i} \quad = \quad \frac{\partial f_e^{-1}}{\partial e_i}\cdot\left(v_{i-1}-f_v(\alpha_{1i})-z_{2i}\cdot\frac{\partial f_v}{\partial y_i^v}(\alpha_{1i}+\epsilon z_{2i})\right) \tag{78}$$

By designing the virtual control α_{1i} as (67), which is a function depending on (p_{i-1},p_i,v_{i-1}), we get

$$\dot{z}_{1i} \quad = \quad -c_i z_{1i}+h_{z_{2i}}z_{2i} \tag{79}$$

where $h_{z_{2i}}=-\frac{\partial f_e^{-1}}{\partial e_i}(e_i)\cdot\frac{\partial f_v}{\partial y_i^v}(\alpha_{1i}+\epsilon z_{2i})$. Note that, as stated in Chapter 2.3.2 of the book Krstic et al. (1995), by the implicit function theorem, a couple of necessary conditions for the existence of (67) are

$$\frac{\partial f_e^{-1}}{\partial e_i}\neq 0, \quad \frac{\partial f_v}{\partial y_i^v}\neq 0 \tag{80}$$

which are naturally satisfied by the calculation of the relevant partial derivatives.

Step 2 of Vehicle i. Similarly, take time-derivative of z_{2i} of (65) along (36), and use (66)

$$\dot{z}_{2i} \quad = \quad \dot{y}_i^v-\dot{\alpha}_{1i}=\frac{\partial f_v^{-1}}{\partial v_i}\cdot f_a(\alpha_{2i})+z_{3i}\frac{\partial f_v^{-1}}{\partial v_i}\frac{\partial f_a}{\partial y_i^a}(\alpha_{2i}+\epsilon z_{3i})-\frac{\partial\alpha_{1i}}{\partial p_{i-1}}v_{i-1}-\frac{\partial\alpha_{1i}}{\partial p_i}v_i-\frac{\partial\alpha_{1i}}{\partial v_{i-1}}a_{i-1} \tag{81}$$

$$= \quad -c_i z_{2i}+h_{z_{3i}}z_{3i} \tag{82}$$

where $h_{z_{3i}}=\frac{\partial f_v^{-1}}{\partial v_i}(v_i)\cdot\frac{\partial f_a}{\partial y_i^a}(\alpha_{2i}+\epsilon z_{3i})$ and α_{2i} is designed as (68).

Step 3 of Vehicle i. Take time-derivative of z_{3i} of (66) along (37), and use (70)-(71)

$$\dot{z}_{3i}=\dot{y}_i^a-\dot{\alpha}_{2i}=\frac{\partial f_a^{-1}}{\partial a_i}\cdot(b_iu_i+\varphi_i^T\theta_i)-\frac{\partial\alpha_{2i}}{\partial a_{i-1}}(b_{i-1}u_{i-1}+\varphi_{i-1}^T\theta_{i-1})-\frac{\partial\alpha_{2i}}{\partial p_{i-1}}v_{i-1}-\frac{\partial\alpha_{2i}}{\partial p_i}v_i-\frac{\partial\alpha_{2i}}{\partial v_{i-1}}a_{i-1}-\frac{\partial\alpha_{2i}}{\partial v_i}a_i$$

$$=-c_iz_{3i}-\frac{\partial f_a^{-1}}{\partial a_i}b_i\tilde{\varrho}_i\alpha_{3i}+\frac{\partial f_a^{-1}}{\partial a_i}\varphi_i^T\tilde{\theta}_i-\frac{\partial\alpha_{2i}}{\partial a_{i-1}}\tilde{b}_{i-1}u_{i-1}-\frac{\partial\alpha_{2i}}{\partial a_{i-1}}\varphi_{i-1}^T\tilde{\theta}_{i-1} \tag{83}$$

Lyapunov-based Stability Analysis.

Build Lyapunov-candidate for vehicle i as

$$V_i \quad = \quad \frac{1}{2}z_{1i}^2+\frac{1}{2}z_{2i}^2+\frac{1}{2}z_{3i}^2+\frac{|b_i|}{2\gamma_i}\tilde{\varrho}_i^2+\frac{1}{2\gamma_{i-1}}\tilde{b}_{i-1}^2+\frac{1}{2\gamma_{i-1}}\tilde{\theta}_{i-1}^T\tilde{\theta}_{i-1}+\frac{1}{2\gamma_i}\tilde{\theta}_i^T\tilde{\theta}_i \tag{84}$$

Taking time derivative of (84) along the dynamics of the closed-loop system (79), (82) and (83), we have

$$\begin{aligned}
\dot{V}_i =& z_{1i}\left(-c_i z_{1i} + h_{z_{2i}} z_{2i}\right) + z_{2i}\left(-c_i z_{2i} + h_{z_{3i}} z_{3i}\right) \\
&+ z_{3i}\left(-c_i z_{3i} - \frac{\partial f_a^{-1}}{\partial a_i} b_i \tilde{\varrho}_i \alpha_{3i} + \frac{\partial f_a^{-1}}{\partial a_i}\varphi_i^T \tilde{\theta}_i - \frac{\partial \alpha_{2i}}{\partial a_{i-1}}\tilde{b}_{i-1} u_{i-1} - \frac{\partial \alpha_{2i}}{\partial a_{i-1}}\varphi_{i-1}^T \tilde{\theta}_{i-1}\right) \\
&- \frac{|b_i|}{\gamma_i}\tilde{\varrho}_i \dot{\tilde{\varrho}}_i - \frac{1}{\gamma_{i-1}}\tilde{b}_{i-1}\dot{\tilde{b}}_{i-1} - \frac{1}{\gamma_{i-1}}\tilde{\theta}_{i-1}^T \dot{\tilde{\theta}}_{i-1} - \frac{1}{\gamma_i}\tilde{\theta}_i^T \dot{\tilde{\theta}}_i \qquad (85) \\
=& -\frac{c_i}{2} z_{1i}^2 - \frac{c_i}{2}\left(z_{1i} - \frac{h_{z_{2i}}}{c_i} z_{2i}\right)^2 - \left(\frac{c_i}{4} - \frac{h_{z_{2i}}^2}{2c_i}\right) z_{2i}^2 - \frac{c_i}{2} z_{2i}^2 - \frac{c_i}{4}\left(z_{2i} - \frac{2h_{z_{3i}}}{c_i} z_{3i}\right)^2 - \left(\frac{c_i}{2} - \frac{h_{z_{3i}}^2}{c_i}\right) z_{3i}^2 - \frac{c_i}{2} z_{3i}^2 \qquad (86) \\
&- \frac{|b_i|}{\gamma_i}\tilde{\varrho}_i\left(\dot{\tilde{\varrho}}_i + \gamma_i \mathrm{sgn}(b_i)\frac{\partial f_a^{-1}}{\partial a_i}\alpha_{3i} z_{3i}\right) - \frac{1}{\gamma_{i-1}}\tilde{b}_{i-1}\left(\dot{\tilde{b}}_{i-1} + \gamma_{i-1}\frac{\partial \alpha_{2i}}{\partial a_{i-1}} u_{i-1} z_{3i}\right) \\
&- \frac{1}{\gamma_{i-1}}\tilde{\theta}_{i-1}^T\left(\dot{\tilde{\theta}}_{i-1} + \gamma_{i-1}\varphi_{i-1}\frac{\partial \alpha_{2i}}{\partial a_{i-1}} z_{3i}\right) - \frac{1}{\gamma_i}\tilde{\theta}_i^T\left(\dot{\tilde{\theta}}_i - \gamma_i \varphi_i \frac{\partial f_a^{-1}}{\partial a_i} z_{3i}\right) \qquad (87) \\
\leq& -\frac{c_i}{2}(z_{1i}^2 + z_{2i}^2 + z_{3i}^2) - \frac{|b_i|}{\gamma_i}\tilde{\varrho}_i\left(\dot{\tilde{\varrho}}_i + \gamma_i \mathrm{sgn}(b_i)\frac{\partial f_a^{-1}}{\partial a_i}\alpha_{3i} z_{3i}\right) - \frac{1}{\gamma_{i-1}}\tilde{b}_{i-1}\left(\dot{\tilde{b}}_{i-1} + \gamma_{i-1}\frac{\partial \alpha_{2i}}{\partial a_{i-1}} u_{i-1} z_{3i}\right) \\
&- \frac{1}{\gamma_{i-1}}\tilde{\theta}_{i-1}^T\left(\dot{\tilde{\theta}}_{i-1} + \gamma_{i-1}\varphi_{i-1}\frac{\partial \alpha_{2i}}{\partial a_{i-1}} z_{3i}\right) - \frac{1}{\gamma_i}\tilde{\theta}_i^T\left(\dot{\tilde{\theta}}_i - \gamma_i \varphi_i \frac{\partial f_a^{-1}}{\partial a_i} z_{3i}\right) \qquad (88)
\end{aligned}$$

where c_i is selected to meet $c_i^2 \geq 2\max\{\|h_{z_{2i}}^2\|_\infty, \|h_{z_{3i}}^2\|_\infty\}$, as $h_{z_{2i}}$ and $h_{z_{3i}}$ for $i = 1, \cdots, n-1$ are bounded.

Then build Lyapunov candidate for the closed-loop systems of the whole vehicle platoon as follows,

$$V = \sum_{i=1}^{n}\left(\frac{1}{2}z_{1i}^2 + \frac{1}{2}z_{2i}^2 + \frac{1}{2}z_{3i}^2\right) + \sum_{i=1}^{n}\frac{|b_i|}{2\gamma_i}\tilde{\varrho}_i^2 + \sum_{i=1}^{n-1}\frac{1}{2\gamma_i}\tilde{b}_i^2 + \sum_{i=1}^{n}\frac{1}{2\gamma_i}\tilde{\theta}_i^T\tilde{\theta}_i \qquad (89)$$

From (88), the time derivative of V is calculated as

$$\begin{aligned}
\dot{V} \leq& -\sum_{i=1}^{n}\frac{c_i}{2}(z_{1i}^2 + z_{2i}^2 + z_{3i}^2) - \sum_{i=1}^{n}\frac{|b_i|}{\gamma_i}\tilde{\varrho}_i\left(\dot{\tilde{\varrho}}_i + \gamma_i \mathrm{sgn}(b_i)\frac{\partial f_a^{-1}}{\partial a_i}\alpha_{3i} z_{3i}\right) - \sum_{i=1}^{n-1}\frac{1}{\gamma_i}\tilde{b}_i\left(\dot{\tilde{b}}_i + \gamma_i\frac{\partial \alpha_{2,i+1}}{\partial a_i} u_i z_{3,i+1}\right) \\
&- \sum_{i=1}^{n-1}\frac{1}{\gamma_i}\tilde{\theta}_i^T\left(\dot{\tilde{\theta}}_i + \gamma_i\varphi_i\left(\frac{\partial \alpha_{2,i+1}}{\partial a_i} z_{3,i+1} - \frac{\partial f_a^{-1}}{\partial a_i} z_{3i}\right)\right) - \frac{1}{\gamma_n}\tilde{\theta}_n^T\left(\dot{\tilde{\theta}}_n - \gamma_n\varphi_n\frac{\partial f_a^{-1}}{\partial a_n} z_{3n}\right) \qquad (90)
\end{aligned}$$

By applying parameter update laws (72)-(75) to cancel parameter estimation error terms in (90), it is apparent $\dot{V}$ is non-positive as

$$\dot{V} \leq -\sum_{i=1}^{n}\frac{c_i}{2}(z_{1i}^2 + z_{2i}^2 + z_{3i}^2) \qquad (91)$$

Thus z_{1i}, z_{2i}, z_{3i} of (64)-(66) are bounded, which renders the boundedness of y_i^e, y_i^v, y_i^a. Then state constraints (14)-(16) are observed from (32)-(34). By LaSalle-Yoshizawa theorem, (12)-(13) are ensured. Theorem 2 is proved.

Combing the state constraint (14) with Assumption 1, the spacing error is restricted to a bounded interval such that

$$\underline{e} - \overline{e} < e_i(t) - e_i^r < \overline{e} - \underline{e} \Leftrightarrow |e_i(t) - e_i^r| < \overline{e} - \underline{e} \qquad (92)$$

Thus the perturbation in the inter-vehicle spacing from its desired value can not infinitely grow from one vehicle to its follower even when the platoon has an infinite number of vehicles.

Remark 3: Note that in the control scheme above, the local controller (41)-(45) or (67)-(71) of the ith vehicle only utilizes the information of its immediate predecessor $i-1$, while the local parameter estimator (46)-(49) or (72)-(75) of the ith vehicle only utilizes the information of its closest successor $i+1$. Therefore the V2V communication style in this paper is the simple "bi-directional" (BD) type as shown in Fig. 1. In contrast to more complex communication modes, the BD type neither requires the leading vehicle's data to be transmitted to every following vehicle, nor requires one vehicle to collect information from all vehicles ahead or back. Such short-distance and low-volume data transmission is easy to implement in practice, and may significantly reduce the effect of communication delay and dropout (which is common in long-distance and high-volume data transmission). In fact, in this paper, if one vehicle is able to measure the states (position-velocity-acceleration) of its nearest predecessor and successor by senors (which is not difficult by modern sensing technology), the distributed control can be simplified to decentralized control without communication. Nevertheless, the above merit may not be accompanied by the popular MPC method with state constraint. As claimed in Assumption 2.1 of Zhou et al. (2017), the MPC scheme requires every following vehicle to be able to monitor the leading vehicle's real-time behavior through the complicated communication style.

4. Simulation

Consider a platoon of CAVs driving in equilibrium, that is, all vehicles follow a leading vehicle $i=0$ with the same steady-state velocity $v_i = v_0$, while maintaining an ideal spacing $e_i = p_{i-1} - p_i - l_{i-1} = e_i^r$ between any two consecutive vehicles. At some point, let us apply the 'hand of God' and 'kick' the leading vehicle out of equilibrium. The disturbance also forces subsequent vehicles to deviate from their equilibria. Over time, the velocity and spacing of all vehicles fluctuate. The 'hand of God' may come from reality. For example, in a real traffic environment, the leading vehicle alternatively accelerates or decelerates to adapt to different road conditions, producing a time-varying reference velocity $v_0(t)$. As other vehicles in the stream are expected to track the time-varying speed, the platoon's steady-state is continuously changing. In the simulation, our control scheme is tested to verify whether the deviation from the platoon equilibrium is bounded and vanishes over time, which means that the platoon can return to the original steady state or reach a new steady state after a finite time.

In the simulation, we consider a platoon of six CAVs with one being the leading vehicle. The third-order nonlinear vehicular dynamics is listed as (4)-(7). Plant parameters are chosen from practical range in Table 2: $m_i = 1000kg$, $K_{di} = 0.3$, $d_{mi} = 100$ for $i = 1,2,3,4,5$. Considering the vehicle heterogeneity in a platoon, we assume $\tau_i = 0.5$ for $i = 1,3$ whereas $\tau_i = 0.3$ for $i = 2,4,5$. The inertial time lag τ_i is assumed to be unknown which results in three unknown parameters for each vehicle such that $b_i = \frac{1}{\tau_i}$, $\varrho_i = \tau_i$ and $\theta_i = -\frac{1}{\tau_i}$. The length for six vehicles are all equal to $l_i = 5m$. The desired inter-vehicle distance is set as $e_i^r = 50m$. The state constraints are listed as follows. The minimum and maximum inter-vehicle distance are $\underline{e} = 49.9m$ and $\overline{e} = 50.1m$. The lowest and highest speed limits on the highway are $\underline{v} = 9m/s$ and $\overline{v} = 31m/s$. The largest deceleration and acceleration are $-\underline{a} = -2.1m/s^2$ and $\overline{a} = 2.1m/s^2$. The time-varying reference velocity and acceleration of the leading vehicle is governed by the time-varying reference input $u_0(t)$ below,

$$u_0(t) = \begin{cases} 0.1, & t \in [10,20) \\ -0.1, & t \in [20,30] \\ -0.2, & t \in [40,50) \\ 0.2, & t \in [50,60] \\ 0.2, & t \in [70,80) \\ -0.2, & t \in [80,90] \\ -0.1, & t \in [100,110) \\ 0.1, & t \in [110,120] \\ 0, & \text{else} \end{cases} \tag{93}$$

Now we test the control scheme to deal with both unknown parameters and state constraints in Section 3.2. The initial estimates of the unknown parameters are set as $\hat{b}_i(0) = 5$, $\hat{\varrho}_i(0) = 0$, $\hat{\theta}_i(0) = -5$, which are far from their unknown real values. The results are shown in Figs. 3-6. From Fig. 3, it is obvious that the following vehicles' velocities track the leading vehicle's time-varying velocity, whether the leading vehicle accelerates or decelerates.

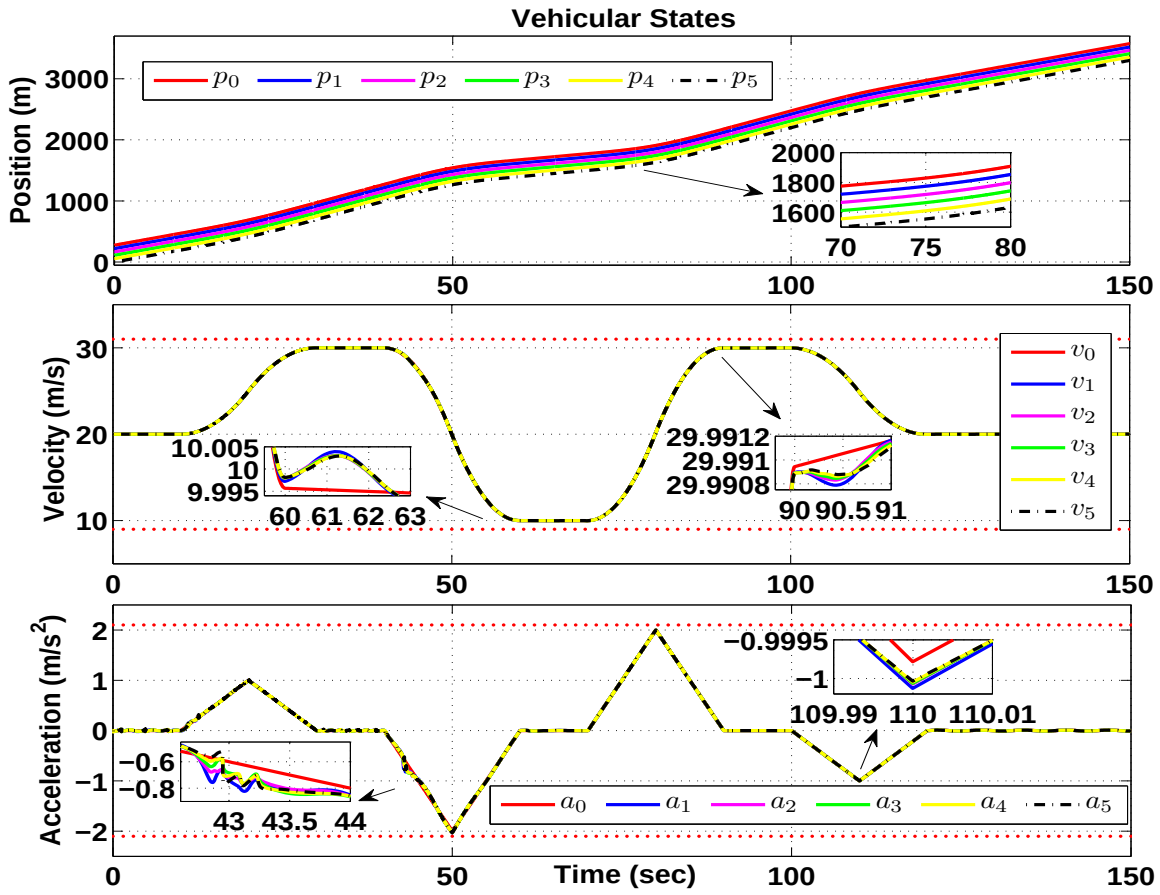

Figure 3: Vehicular State under Parametric Uncertainty and State Constraint by Backstepping

The position curves are almost parallel with no collision. The velocity and acceleration of all vehicles abide by the red dash line constraints. In Fig. 4, the inter-vehicle distances are bounded and converge to the desired value in a finite time, and the red dash line constraints are not violated. Relative velocities are also bounded and converge to zero in a finite time. Figs. 5-6 show the accurate estimations of the unknown three parameters, although initial estimation errors are large.

Another important criterion to evaluate the performance of a vehicle platoon is the string stability. The analysis of string stability usually depends on the transfer function in Laplace domain. This method could be employed for simplified linear vehicular dynamics. However, as stated in Remark 1, when the parameters are uncertain and the nonlinear plants are unable to be linearized, the transfer function approach for linear systems cannot be applied since nonlinear systems cannot be represented by Laplace transformation.

As stated on Page 151 of Swaroop et al. (2001), in the presence of parametric uncertainty, the requirement of string stability in its rigorous definition $\left(i.e., \left\| \frac{e_i(s)-e_i^r(s)}{e_{i-1}(s)-e_{i-1}^r(s)} \right\|_{\mathcal{H}_\infty} \leq 1, \text{ Theorem 1 of Ploeg et al. (2014)}\right)$ is very stringent. In fact, our control scheme is unable to ensure the strict string stability. However, as clarified by Swaroop et al. (2001), under the parametric uncertainty, the string stability is relaxed such that the errors in spacing are bounded not only in time but also uniformly in vehicle index. This relaxed string stability is ensured by our control scheme (as shown in the proofs of Theorems 1 and 2).

Most importantly, the physical meaning of the string stability is that the deviation of the inter-vehicular distance from its desired value does not amplify upstream from one vehicle to another. The ultimate objective is to prevent the infinite propagation of the spacing error in a traffic stream (which is assumed to consist of an infinite number of vehicles). In this sense, the final goal of string stability is not violated under the state constraints guaranteed by the barrier function, as the spacing error of each vehicle is limited to a bounded interval as shown in Eq. (92). This is also confirmed in Fig. 4, the inter-vehicle spacing do not go beyond the red dash line. In other words, the prevention of spacing error from infinitely amplifying is established by the state constraint.

Furthermore, one of the well-known advantages of the backstepping method is that the transient performance could be improved by adjusting design coefficients c_i and γ_i. In simulation, these design coefficients are carefully

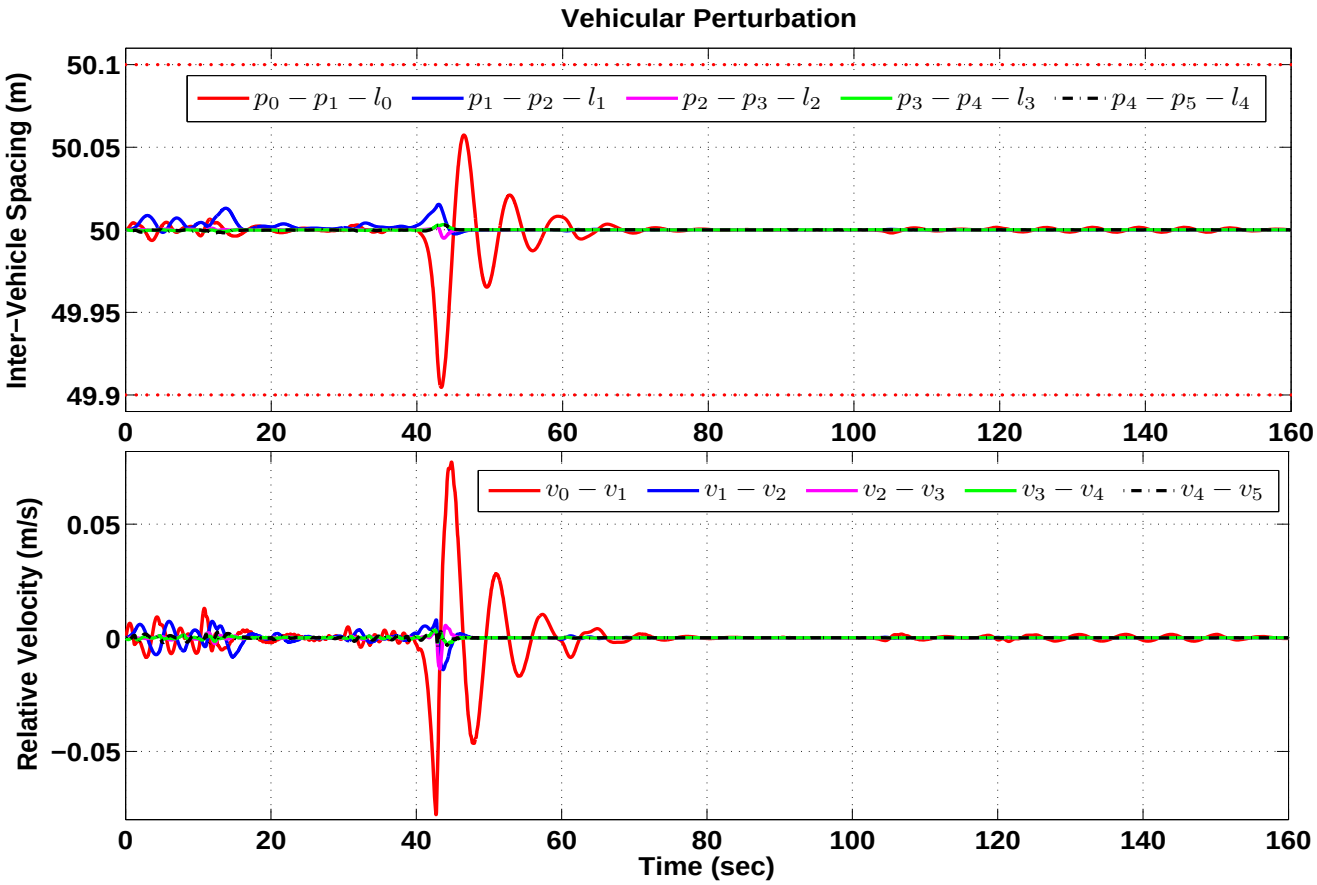

Figure 4: Vehicular Perturbation under Parametric Uncertainty and State Constraint by Backstepping

selected (through trial and error) to regulate the spacing error not to amplify.

5. Conclusion

This paper proposes a distributed control approach for a platoon of connected and automated vehicles (CAVs) that are modeled by a general class of third-order nonlinear systems with parametric uncertainty and full-state constraint. Compared with second-order or third-order linear models that are widely used in the literature, the third-order nonlinear systems not only more accurately represent the vehicle internal dynamics, but also overcome the linearization's weakness that requires perfect knowledge of the plant parameters (as elaborated in Remarks 1). The control algorithm can handle uncertainties in all vehicular parameters including both plant parameters and control coefficients. Another merit is that the practical constraints on vehicular full-state are taken into account. Different from the classic MPC, the proposed barrier-function-based backstepping method is not limited to linear systems and does not require complicated data communication (as elaborated in Remark 3). In the proposed control scheme, nonlinearities are handled, uncertain parameters are estimated on-line, state constraints are obeyed, and the tracking control objectives are accomplished. Simulation studies verify the feasibility of the proposed control design.

In the present paper, the state constraint is addressed, whereas the input constraint is not taken into account in the platoon control problem. In the future, a development of adaptive control algorithm to deal with both constraints on state and input is an interesting topic worthy of investigation.

Acknowledgements

This study is supported by Singapore Ministry of Education Academic Research Fund Tier 2 MOE2017-T2-1-029.

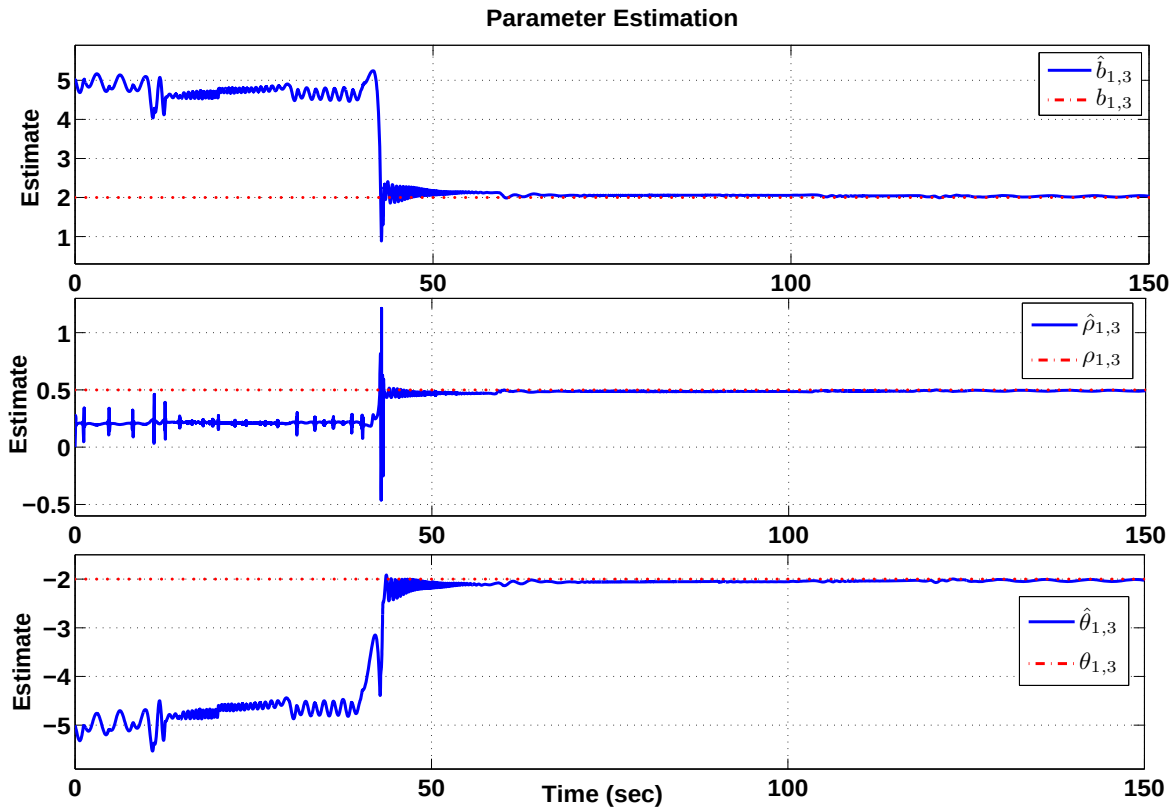

Figure 5: Parameter Estimation of Vehicle 1 and 3

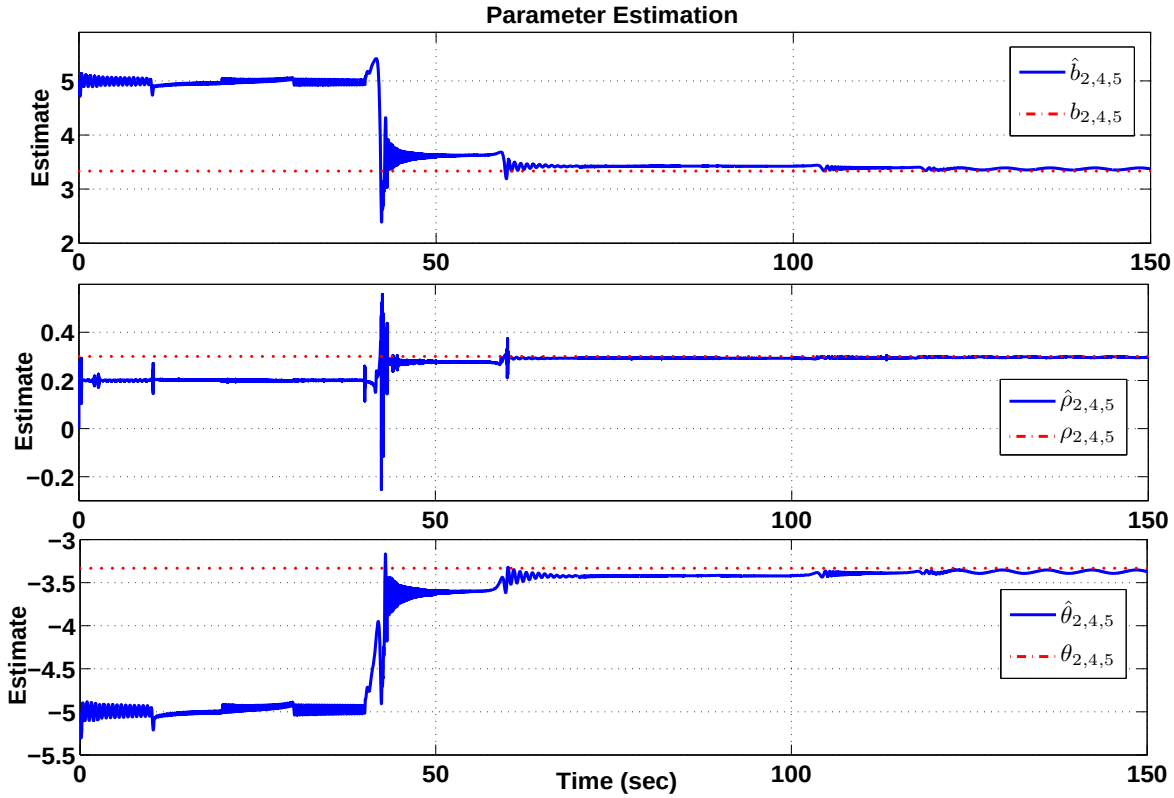

Figure 6: Parameter Estimation of Vehicle 2, 4 and 5

References

Bian, Y., Zheng, Y., Ren, W., Li, S-E., Wang, J., Li, K-Q. 2019. Reducing time headway for platooning of connected vehicles via V2V communication, *Transportation Research Part C: Emerging Technologies*, vol. 102, pp. 87-105.

Besselink, Bart. and Johansson, K. H. 2017. String stability and a delay-based spacing policy for vehicle platoons subject to disturbances. *IEEE Transactions on Automatic Control*, vol. 62, pp. 4376-4391.

Chehardoli, H., Ghasemi, A., 2018. Adaptive centralized/decentralized control and identification of 1-D heterogeneous vehicular platoons based on constant time headway policy, *IEEE Transactions on Intelligent Transportation Systems*, vol. 19, pp. 3376 - 3386.

Chen, N., Wang. M., Alkim, T., and Arem, B., 2018. A robust longitudinal control strategy of platoons under model uncertainties and time delays, *Journal of Advanced Transportation*, https://doi.org/10.1155/2018/9852721.

Feng, Y., Yu, C., Liu, H. X., 2018. Spatiotemporal intersection control in a connected and automated vehicle environment, *Transportation Research Part C: Emerging Technologies*, vol. 89, pp. 364-383, 2018.

Filho, C. M., Terra, M. H., Wolf, D. F., 2017. Safe optimization of highway traffic with robust model predictive control-based cooperative adaptive cruise control, *IEEE Transactions on Intelligent Transportation Systems*, vol. 18, pp. 3193-3203.

Gao, F., Hu, X., Li, S-E., Li, K-Q, Sun, Q., 2018. Distributed adaptive sliding mode control of vehicular platoon with uncertain interaction topology, *IEEE Transactions on Industrial Electronics*, 65, 6352-6361.

Ge., J-I. and Orosz, G. 2014. Dynamics of connected vehicle systems with delayed acceleration feedback, *Transportation Research Part C*, vol. 46, pp. 46-64.

Gong, S., Du, L., 2018. Cooperative platoon control for a mixed traffic flow including human drive vehicles and connected and autonomous vehicles, *Transportation Research Part B: Methodological*, vol. 116, pp. 25-61.

Gong, S., Shen J., Du, L., 2016. Constrained optimization and distributed computation based car following control of a connected and autonomous vehicle platoon, *Transportation Research Part B: Methodological*, vol. 94, pp. 314-334.

Guo, G. and Yue, W., 2012. Autonomous platoon control allowing range-limited sensors, *IEEE Transactions on Vehicular Technology*, vol. 61, pp. 2901-2912, 2012.

Krstic, M., Kanellakopoulos, I., Kokotovic, P., 1995. *Nonlinear and adaptive control design*, John Willey, New York, 1995

Li, S., Yang, L. and Gao, Z., 2015. Coordinated cruise control for high-speed train movements based on a multi-agent model, *Transportation Research Part C: Emerging Technologies*, vol. 56, pp. 281-292, Jul. 2015.

Li, S., Yang, L., Li, K. and Gao, Z., 2014. Robust sampled-data cruise control scheduling of high speed train, *Transportation Research Part C: Emerging Technologies*, vol. 46, pp. 274-283, 2014.

Li, S-E., Zheng, Y., Li, K-Q., Wu, Y., Gao, F., Zhang, H-W., Hedrick, J. K., 2017a. Dynamical modeling and distributed control of connected and automated vehicles: challenges and opportunities, *IEEE Intelligent Transportation Systems Magazine*, vol. 9, pp. 46-58, 2017.

Li, S-E., Gao, F., Li, K., Wang, L-Y., You, K. and Cao, D., 2017b. Robust longitudinal control of multi-vehicle systems a distributed h-infinity method, *IEEE Transactions on Intelligent Transportation Systems*, DOI: 10.1109/TITS.2017.2760910, 2017

Li, S-E., Qin, X., Li, K-Q., Wang, J., Xie, B., 2017c. Robustness analysis and controller synthesis of homogeneous vehicular platoons with bounded parameter uncertainty, *IEEE/ASME Transactions on Mechatronics*, vol. 22, pp. 1014-1025, 2017.

Li, Y., Tang, C., Li, K., Peet, S., He, X., Wang, Y. 2018. Nonlinear finite-time consensus-based connected vehicle platoon control under fixed and switching communication topologies. *Transportation Research Part C: Emerging Technologies*, vol. 93, pp. 525-543.

Ploeg, J., Wouw, N. and Nijmeijer, H., 2014. Lp string stability of cascaded systems: Application to vehicle platooning. *IEEE Transactions on Control Systems Technology*, vol. 22, pp. 786-793, 2014.

Petrillo, A., Salvi, A., Santini, S., Valente, A. S., 2018. Adaptive multi-agents synchronization for collaborative driving of autonomous vehicles with multiple communication delays, *Transportation Research Part C: Emerging Technologies*, vol. 86, pp. 372-392, 2018.

Salvi, A., Santini, S., Valente, A. S., 2017. Design, analysis and performance evaluation of a third order distributed protocol for platooning in the presence of time-varying delays and switching topologies, *Transportation Research Part C: Emerging Technologies*, vol. 80, pp. 360-383, 2017

Sheikholeslam, S. and Desoer, C. A., 1993. Longitudinal control of a platoon of vehicles with no communication of lead vehicle information: a system level study, *IEEE Transactons Vehicular Technology*, vol. 42, no. 4, pp. 546-554, 1993.

Sun, X., Yin, Y., 2019. Behaviorally stable vehicle platooning for energy savings, *Transportation Research Part C: Emerging Technologies*, vol. 99, pp. 37-52.

Ioannou, P. A. and Chien, C. C., 1993. Autonomous Intelligent Cruise Control, *IEEE Transactons Vehicular Technology*, vol. 42, pp. 657-672, 1993.

Swaroop, D., Hedrick, J. K., Chien, C. C. and Ioannou, P., 1994. Comparison of spacing and headway control laws for automatically controlled vehicles, *Vehicle System Dynamics*, vol. 23, pp. 597625, 1994.

Godbole, D. N. and Lygeros, J., 1994. Longitudinal control of the lead car of a platoon, *IEEE Transactons Vehicular Technology*, vol. 43, pp. 1125-1135, 1994.

Swaroop, D., Hedrick, J. K., and Choi, S. B., 2001. Direct adaptive longitudinal control of vehicle platoons, *IEEE Transactons Vehicular Technology*, vol. 50, no. 1, pp. 150-161, 2001.

Wang, M., Daamen, W., Hoogendoorn, S., and Arem, B., 2014a. Rolling horizon control framework for driver assistance systems. Part II: Cooperative sensing and cooperative control, *Transportation Research Part C: Emerging Technologies*, 40, 290-311.

Wang, M., Daamen, W., Hoogendoorn, S., and Arem, B., 2014b. Rolling horizon control framework for driver assistance systems. Part I: Mathematical formulation and non-cooperative systems, *Transportation Research Part C: Emerging Technologies*, 40, 271-289.

Zhai, C., Liu, Y., Luo, F., 2018. A switched control strategy of heterogeneous vehicle platoon for multiple objectives with state constraints, *IEEE Transactions on Intelligent Transportation Systems*, DOI: 10.1109/TITS.2018.2841980.

Zheng, Y., Li, S-E., Li, K-Q., Borrelli, F., Hedrick, J-K., 2017a. Distributed model predictive control for heterogeneous vehicle platoons under unidirectional topologies, *IEEE Transactions on Control Systems Technology*, 25, 899-910.

Zheng, Y., Li, S-E., Li, K-Q., Ren, W., 2017b. Platooning of connected vehicles with undirected topologies: robustness analysis and distributed h-infinity controller synthesis, *IEEE Transactions on Intelligent Transportation Systems*, vol. 19, pp. 1353-1364.

Zhou, Y., Ahn, S., Chitturi, M., Noyce D. A., 2017. Rolling horizon stochastic optimal control strategy for ACC and CACC under uncertainty, *Transportation Research Part C: Technologies*, 83, 61-76.

Zhu, Y., Krstic, M., Su, H., 2018a. Adaptive global stabilization of uncertain multi-input linear time-delay systems by PDE full-state feedback, *Automatica*, vol. 96, pp. 270-279, 2018.

Zhu, Y., Krstic, M., Su, H., 2018b. PDE boundary control of multi-input LTI systems with distinct and uncertain input delays, *IEEE Transactions on Automatic Control*, vol. 63, pp. 4270-4277, 2018.

Zhu, Y., Krstic, M. and Su, H., 2017. Adaptive output feedback control for uncertain linear time-delay systems, *IEEE Transactions on Automatic Control*, vol. 62, no. 2, pp. 545-560, 2017

Zhu, Y., Su, H., Krstic, M., Adaptive backstepping control of uncertain linear systems under unknown actuator delay, *Automatica*, vol. 54, pp. 256-265, 2015.

Zhu, Y., Zhu, F., 2018. Distributed adaptive longitudinal control for uncertain third-order vehicle platoon in a networked environment, *IEEE Transactons Vehicular Technology*, 67, 9183-9196.

Zhu, F., Ukkusuri, S. V., 2017. Efficient and fair system states in dynamic transportation networks, *Transportation Research Part B: Methodological*, vol. 104, pp. 272-289, 2017

Zhu, F., Ukkusuri, S. V., 2015. A linear programming formulation for autonomous intersection control within a dynamic traffic assignment and connected vehicle environment, *Transportation Research Part C: Emerging Technologies*, vol. 55, pp. 363-378, 2015.

Zhu, Y. H., Zhao, D., Zhong, Z., 2018. Adaptive optimal control of heterogeneous CACC system with uncertain dynamics. *IEEE Transactions on Control Systems Technology*, DOI: 10.1109/TCST.2018.2811376.